Asian Journal of Chemistry Vol. 22, No. 2 (2010), 1462-1478

Investigation of Turbid Water Characteristics and Its Control at a Slag Landfill Located by the Seashore

HWAN LEE†, CHOLHO LEE‡ and YOON-JIN LEE*
Department of Environmental Engineering, Cheongju University, 36, Naedok-dong, Sangdang-gu, Cheongju, Chungbuk 360-764, South Korea
E-mail: yjlee@cju.ac.kr

This study was conducted to evaluate the possible cause of the turbidity leaks around the K steel slag landfill located in the republic of Korea and suggest a future counter-plan to mitigate the currents problems of leaching turbid water and control by monitoring the behaviour of the pollutants based on data taken from field surveys and laboratory experiments. The distribution of the turbidity source and possible discharge points were examined through exploration of electric specific resistance and excavation, which observed the behaviour of pollutants and movement closely related to geological characteristics such as base soils and rock constituent. The function of pollutant removal for the existing filtration system and facilities was tested in laboratory scale equipment with brand-new media and excavated media from the field. A more than 98 % removal efficiency of turbidity for both media was achieved with the serial multi-media filtration system. The cutoff function of the bentonite mat was lowered compared to that of the new one, which might be due to the reaction of salt in seawater.

Key Words: Slag, Turbidity, Bentonite, Landfill, Filtration.

INTRODUCTION

Steel production is a crucial foundation industry that intensively influences other industries. Consideration for the green production and elevation of energy efficiency is more emphasized. The steel industry used to result inevitably in various sorts of by-products and waste as well as large useful amounts of products and energy during the manufacturing process. Slag occupies a significant portion of the solid waste generated by the steel industry[1-3]. The substance erupting from slag should be considered as the source of environmental problems.

Ferrous slag is mainly categorized as blast furnace slag, steel slag, alloy steel slag and ferroalloy slag. Blast furnace slag and steel slag contain the main portion of ferrous slag. Iron slag comes from the blast furnace during the iron manufacturing process and has a small portion of iron (< 2 %). Thus, recovery of the metal is not

†Department of Civil, Urban and Geosystem Engineering, Seoul National University, Gwanak 599, Gwanak-ro, Gwanak-gu, Seoul 151-742, South Korea.
‡Research Development Team, Oikos Co., 481-11, Gasan-dong, Gumchun-gu, Daeyungtech Town (8th), Seoul 153-775, South Korea.

a crucial issue for blast furnace slag. Steel slag results from a basic oxygen furnace and electric arc furnace during the steel production process[4]. The typical major compositions of steel slag are calcium oxide (CaO), silicon dioxide (SiO_2) and other substances such as manganesium oxide (MgO), manganese oxide (MnO)[5,6]. Iron and steel slag were not considered harmful waste in terms of the TCLP (toxicity characteristic leaching procedure) criterion concentration from the leaching test according to Proctor *et al.*[7].

Recycling as a raw material for other industries such as cement raw substance or application for road and concrete construction and hydraulic purposes such as stabilization of river banks and dams in the field of civil engineering, which is generally considered the method for consumption of great amounts of iron and steel slag, remains[8-11]. Recently, various experimental researches were conducted on the environmentally favourable application of slag that resulted in environmental treatment, fertilizer production, ground stabilization and brick manufacturing[11-13].

Iron slag is generated with 220-370 kg per unit ton of iron production[7]. Thus, management of the disposal or recycling of this great amount of industrial waste is a crucial issue that must be solved. The problem of mass application and safety still remains for effective recycling/reuse of slag since the fundamental manufacturing method has not changed. Unfortunately, despite these issues, in South Korea, landfills are currently the method most frequently used to dispose of slag.

A slag landfill for slag reclamation discharged from K iron works was constructed in 1995. The establishment of the landfill could solve the problem of slag disposal and is still being used for waste generated during the steel production process. However, another problem has appeared due to the occurrence of turbid water at the seashore caused by leachate discharged from the waste. Thus, supplemental construction has performed, including the installation of a filtration system, to control this pollution problem. However, high turbidity was re-detected in a section after the filtration media construction. Therefore, examination of the cause of the turbid water outbreak and the establishment of a future counter-plan were required. Landfills located at the seashore generally have different hydrologic characteristics compared to those above the ground and the cut-off facility was easily influenced by the exposure effect of seawater. In addition, the character and behaviour of the leachate are considerably affected by the salt concentration and fluctuations in the sea level.

The aim of this study is to examine the cause and possible area that is generating the turbidity leaks and to suggest a complementary plan to control these problems based on laboratory experiment and field measurement data. The behaviour of the pollutant occurrence and movement were observed by a tracer test and excavation. The variation in water quality and hydrologic condition was monitored for the suspicious leak section in the field. The efficiency of the turbidity and iron removal in the laboratory-scale serial filtration system was tested to assess the availability of the existing filtration system in the field.

EXPERIMENTAL

Water quality monitoring: The investigation of the spot for a slag landfill located at the seashore consisted of three processes: water quality monitoring, tracer test and an excavation evaluation to examine the behaviour and movement of the turbidity leaks. The schematic structure for the landfill and the media section is presented in Fig. 1. The landfill was built for the waste produced after iron manufactured at the K steel mill. The section of media layer is a total of 1940.6 m. Slag disposal should be feasible by burying slag in a landfill. But the leachate leak and black turbid water from the slag landfill flowing into the sea became significant problems. A media filtration system was built to prevent these problems. However, after the construction, turbid water was repeatedly drained from some sections. So, an examination of the turbid leak and consideration of a future counter-plan were required. Turbid water was found to be concentrated during the rainy season in the summer period and continued for approximately 1 h for the full tide of the day.

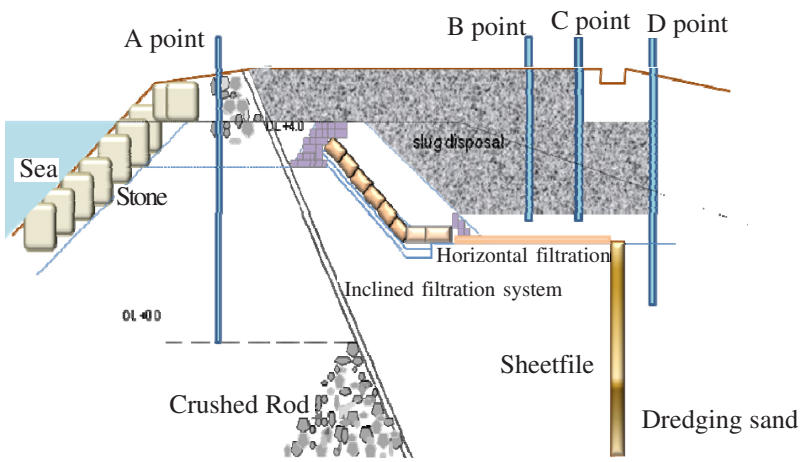

Fig. 1. Schematic diagram of the landfill studied

The monitoring was performed in the field by the following methods: electrical specific resistance was measured by Terrameter SAS 3000C (ABEM) and the data were interpreted with two-dimension adverse estimation. Electrodes were set at an interval of 10 m during the experiment. The investigation was mainly focused on the 440 m of the media layer district, which was an expected potential section of the leachate leak.

The target material for the tracer test was KBr in this experiment because of the high chloride level in this landfill located around the seashore. Initially, 115 mg/L of potassium bromide was injected at observation well D at a depth of 1 m (Fig. 1), and then, the bromide concentration was measured with the passage of time at the A, C, and D observation wells by an Orion aqua-fast II colorimeter.

Successive measurement of the water level was performed for 48 h, including the full and ebb tide for the sea and at the C and D observation wells with an automatic water-level measurement equipment (Hermit 3000). Water samples were collected by a bailer sampler at 1 h intervals. The dissolved oxygen (DO) and pH levels were measured immediately after sampling in the field using a DO meter (YSI model 58), and an electronic pH meter (Omega PHH-103) respectively.

Laboratory test: Samples were taken of the seawater in the field for the indoor experiment, transferred to the laboratory and preserved in a refrigerator under 4 ºC before the tests. Blast furnace slag smashed with a mesh size of 20 to 35 μ was added to induce turbidity in the samples and agitated for 4 h after 1 g/L of FeS (Aldrich) was added. The initial turbidity ranged between 80 and 100 NTU. The water quality for this experiment is presented in Table-1.

TABLE-1
CHARACTERISTICS OF THE WATER SAMPLE FOR THIS EXPERIMENT

pH	7.0 ± 0.2
Water temperature (ºC)	18 ± 5
Turbidity (NTU)	80-100
DO (mg/L)	7.0-7.5
T-Fe (mg/L)	0.9-1.0
Sulfate (mg/L)	± 5

The reactors for evaluation of each media function were made of an acryloyl cylinder, which was manufactured with a 4 cm diameter and 40 cm length. Each reactor was filled with fine sand, activated carbon brought from the field, new activated carbon and non-woven fabric. The pH, DO, turbidity, and iron levels were analyzed after operation for 4 h with the downward flow.

The serial filtration system for studying the media ability and estimating the characteristics of turbidity leaks with the sea tide and the schematic structure for this system are presented in Fig. 2. These reactors were designed to imitate the filtration system in the field. These reactors were filled with, in order, gravel, coarse sand, fine sand, non-woven fabric, activated carbon, non-woven fabric and fine sand from the top counter. Both filtration systems consisted of media from the field and the new media was examined separately. Two reactors, 130 cm length with a diameter of 25 cm, were manufactured. These were operated for 40 days and the operational flow direction was changed every 6 h, upward and downward by turn, four times a day. The flow rate of the influent was regulated with 46 mL/min. The media for the field filtration system were used without specific pretreatment after being removed from the inclined filtration system to minimize the change in the original characteristics of the field media. The conditions such as the filling order of the media and the flow rate were the same as those of the new media.

Samples were taken from each sampling port located between two different media in both filtration systems at 2 h time intervals. The pH, turbidity and DO

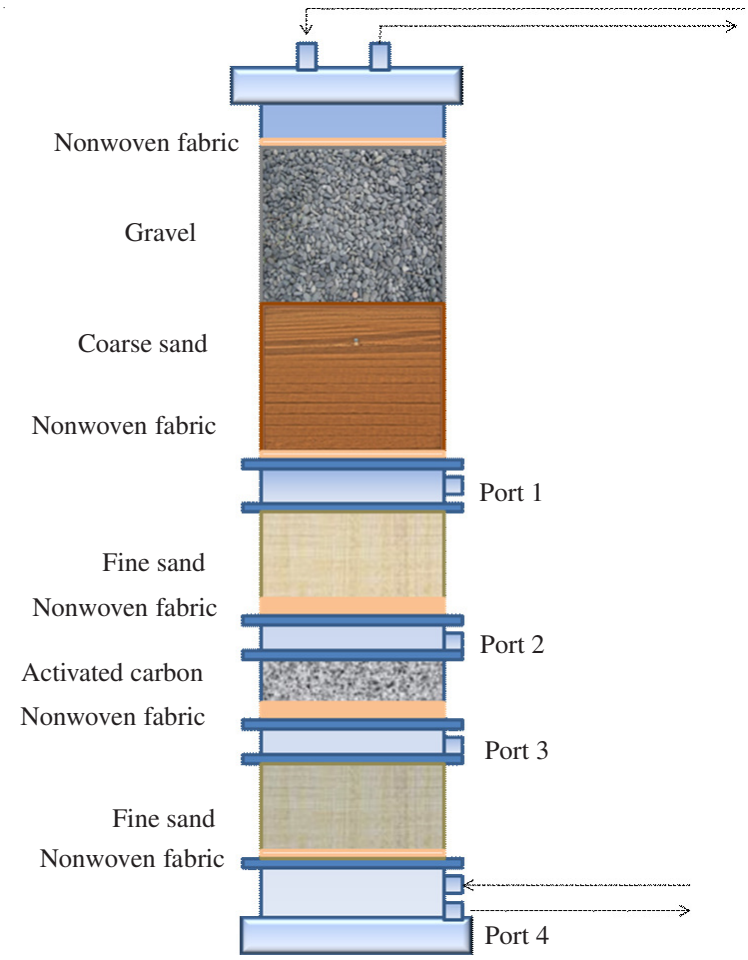

Fig. 2. Multimedia filtration system operated in the laboratory

levels and the levels of iron and sulfate were measured after sampling by the following methods. pH, DO and turbidity were analyzed with a digital pH meter (Corning ion analyzer 250), DO meter (YSI model 58) and turbidimeter (Hach instrument model 2100A), respectively. The sulfate and iron levels were measured by ion chromatography (Dionex 200) and atomic absorption spectrometer (Varian spectra 800), respectively.

The tensile strength measured with two kinds of non-woven fabrics (P565 and Tech 2800, Kungmin Engineering), which were tested for the new product and the one in the inclined filtration system in the field. Samples, which were specimens that were 101.6 mm wide and 203.2 mm long, were pulled with a clamp using an ASTM D 4632-91 with an MTS 810 material test system. The permeability coefficient was determined in the condition with a 4.2 cm water level difference, 78.55 cm^2 of the sample area, 60 s of water permeability time by KS F 2322-00 method.

RESULTS AND DISCUSSION

Turbidity leakage and locomotion: A tracer test with KBr was performed to examine the leakage of the sheet pile and the results are shown in Fig. 3. No bromide was found after 1 h at the D well located inside the cutoff wall. No bromide ions were detected during this experiment at the C wells, which are outside the impervious wall. This result shows leakage through the upper section of sheet file did not occur.

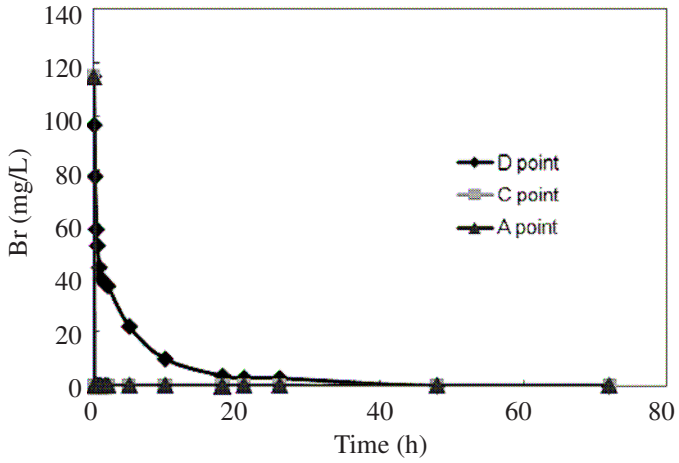

Fig. 3. Variation of bromide ion at three observation wells during tracer test

Distribution of electric specific resistance is presented for the media burying section in Fig. 4. Successful cases of the application of electrical specific resistance have been reported for monitoring of ground water flow and geological structure and controlling for the diffusion of leakage by a cutoff facility in a landfill[14,15]. The main leakage district was predicted to be a station 200 m away from the terminal station of media layered in the direction of the starting point. The ground layer at the starting point of the media layers mostly consisted of belemnite, which has high-water permeability. The fine granular layer of silt sand at the terminal media station should contain pollutants. Large amounts of pollutants were found between -5 and -13 m below the ground level. The low value of the electric specific resistance seen at the upper and lower sections of the horizontal filtration system indicated the possibility of pollutant leakage with the deteriorated media.

The occurrence of black turbid water was confirmed by excavation of the potential leak section, which was expected due to the research on electric specific resistance (Fig. 5). An odour was perceived with the black water during the initial excavation. The black turbid water was converted into white water after exposure to the atmosphere. That might be caused by the formation of calcium sulfate by the reaction with the white deposits of calcium carbonate and sulfate ion that occurred due to the oxidation of the substance that caused the black turbid water. This white water

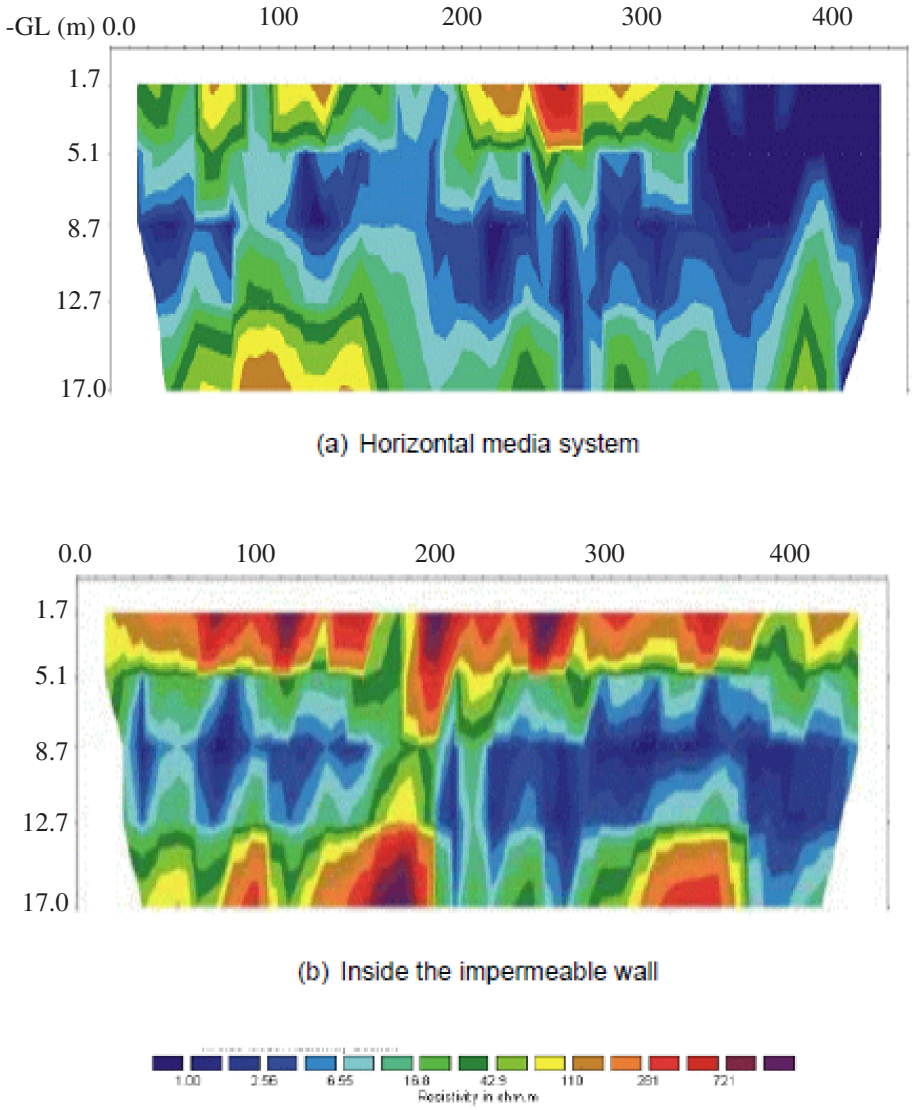

Fig. 4. Distribution of electric specific resistance for the section of horizontal media system and inside the impermeable wall

changed into bluish green after long-term exposure to the atmosphere and inflowing seawater at full tide. The colour change should be caused by the formation of ferric sulfate and ferrous ion with the reaction of FeS and DO. The polluted soil layer was found by the smell of hydrogen sulfide during the excavation. The colour and smell disappeared after 0.5 h of exposure to the atmosphere for this black layer. The black soil was found around the bentonite mat layer.

(a) Black water

(b) White water

(c) Bluish-green water

Fig. 5. Colour change of the leakage after the excavation

Monitoring of water quality variations: The mean level of DO at the C observation well was higher than that of the D observation well (Fig. 6). That might be because a higher exchange reaction with seawater at the C well goes on better than at the D well. The level of DO at the C and D wells changed as the tide changed. This result indicated that water comes in until the head section of the media layer at the horizontal media system at the C well. The DO level was observed to increase at full water and decrease at ebb tide at the C well. The average DO value for seawater, C and D wells was 4.6, 1.0 and 0.9 mg/L, respectively.

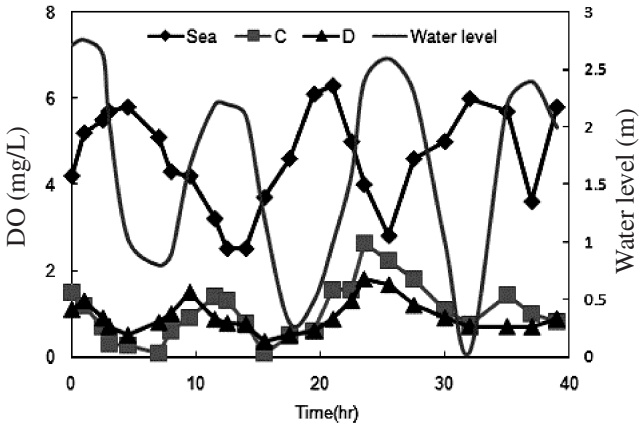

Fig. 6. Variation in DO level with the water level at the sea and C and D wells

The pH was shown to be strongly alkaline, over 10, at C, which was located on the upper side of the horizontal filtration system while the pH for the outside seawater was 8.2 (Fig. 7). The pH levels decreased with full tide for the seawater. The pH value decreased as the level of seawater increased at C. The lower pH value was found when seawater was used as a solvent during a leaching test from steel slag compared to that of distilled water[16].

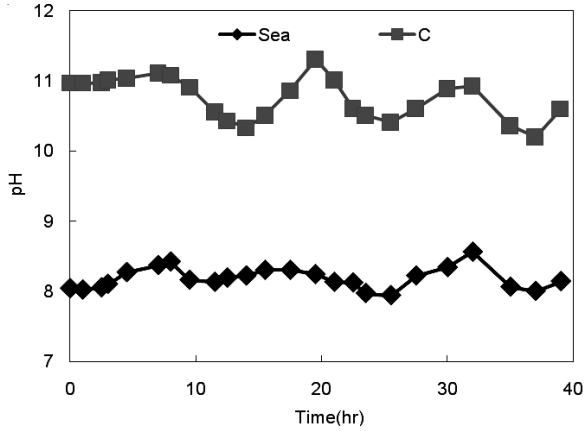

Fig. 7. Variation of pH with the water level at the sea and C wells

The variations of iron and sulfate concentration were measured at B, C and D at full and ebb tide (Fig. 8). A higher concentration of iron and sulfate was detected at high tide compared to that at low tide. The highest difference between the two tides was found at the B well. The level of iron at high tide was 9.6 times higher than that at low tide at the B well. The value of iron was higher from the side of seawater to the inside of the impervious wall and the highest level was 11 mg/L at the D well during high tide.

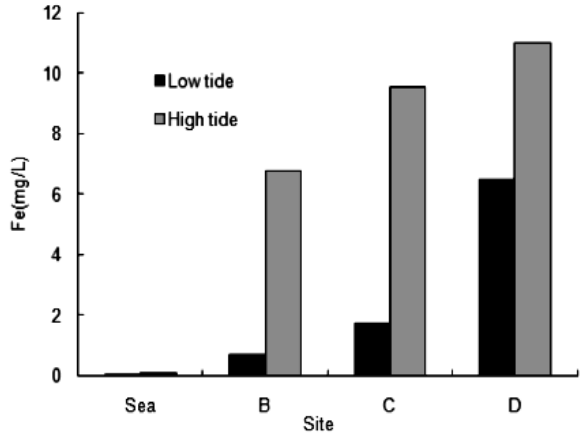

(a) Iron

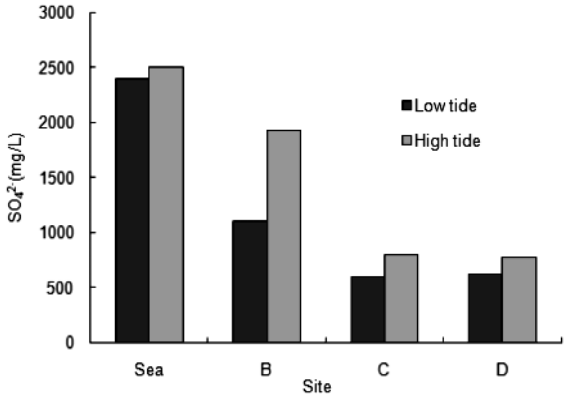

(b) Sulfate

Fig. 8. Variation in iron and sulfate concentrations with low and high tide

The greatest difference in sulfate concentration was found with the tide variations at well B. The concentration of sulfate at full sea was 1.8 times higher than that at ebb tide. Sulfate ions, which exist abundantly in seawater, were detected with a high value at full sea at the well B and the level of sulfate between high and low tides in seawater was similar. The difference between high and low tides at the internal side of the impervious wall was smaller than that outside.

Black turbidity was usually observed 1 h before or after full tide with the smell of hydrogen sulfide and during the summer season in the field. The flow of seawater at full tide might penetrate the cutoff wall and react with the upper layer of the polluted soil. The time needed for the seawater to reach a depth of 2.3 m in the field was estimated to be *ca.* 4 h (the seawater might remain under the horizontal filtration system at the time) and the time needed for the outflow after the reaction with filter media was *ca.* 1 h. So, the total time required from movement and inside penetration of seawater at the full time to outflow after reaction with the upper layer of media was estimated to be 5 h according to our assessment, which corresponds to *ca.* 1 h before or after full tide. The outflow of FeS, turbid-inducing material, could increase by the increase in the reaction velocity with the higher temperature. The situation was also caused by the leachate overflow with the rise of the water level for the inside of the land water and wiping-off of the upper layer media by heavy rains during the summer.

Function assessment of filtration systems: This experiment was conducted to examine the role of each medium buried, such as activated carbon sand and non-woven fabric taken from the field and to evaluate the necessity of exchange work for the existing buried media (Fig. 9a). The highest removal efficiency was shown for the brand-new activated carbon, which was *ca.* 99 % at 3 h. The level of turbidity for the existing activated carbon from the field in the effluent appeared to 2.5 times that of new one at 3 h. The absorption ability of the activated carbon was a little decreased for the field sample compared with the initial state. But the removal efficiency of the activated carbon from field was shown to be more than 97 % after 4 h. It is speculated that filtration does not remarkably greatly for field-activated carbon. The higher order of turbidity removal was registered with the new activated carbon, sand, activated carbon taken from field and non-woven fabric.

The removal of iron increased with the contact time, which was 81, 52, 56 and 62 % for the new activated carbon, activated carbon taken from field, sand and non-woven fabric, respectively, at 1 h and the removal efficiency was enhanced with time (Fig. 9b). The initial removal efficiency of iron during 1 h was somewhat low for both the activated carbon and sand. The iron removal efficiency was shown to be the highest level for the new material of activated carbon, which was 96 % at 4 h. The iron absorption ability was lower than the new one for the activated carbon excavated from field. The removal efficiency of iron at 4 h was 85 % for the activated carbon taken from the field, which was the lowest value of the selected materials. Interestingly, the level of iron removal for non-woven fabric was higher than those of sand and activated carbon, which has been shown to be good efficiency for the turbidity. The higher order of removal efficiency for the iron was shown to be new activated carbon, non-woven fabric, sand and activated carbon from the field.

This experiment was performed to assess the suitability of the current serial filtration system in the field and the decision about the exchange of the present running materials and to evaluate the removal efficiency behaviour with the sea tide

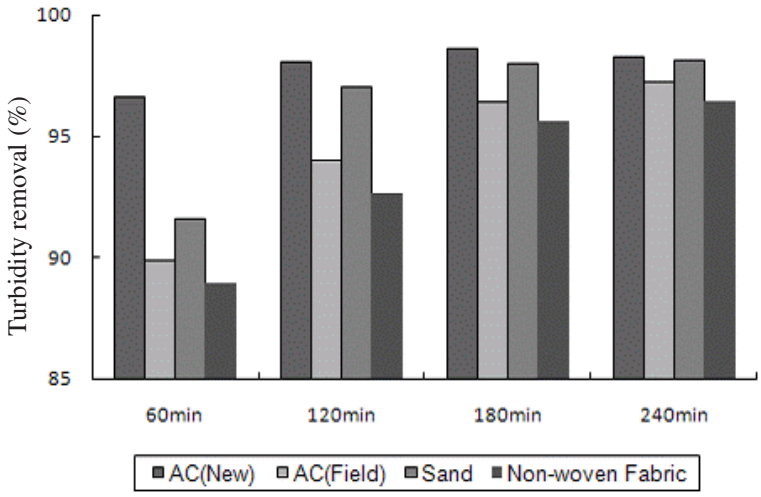

(a) Turbidity

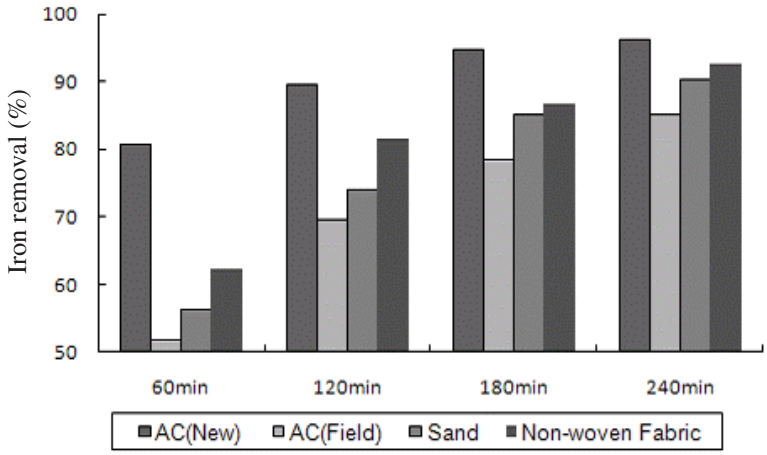

(b) Iron

Fig. 9. Removal efficiency for the turbidity and iron of each medium with time

variation. The two filtration systems operated separately under the same operation conditions were evaluated for the new media and media from the field for the comparison of removal efficiency.

The variation in pH was presented in Fig. 10 at the two filtration systems. The variation in pH through the newly filled media was shown to range between 6.5 and 7.1 until the effluent was discharged. The pH level did not change considerably after the effluent passed through the media during 12 h with down and upflow in the effluent but was a little decreased compared to the initial pH after the effluent was filtered by this media system.

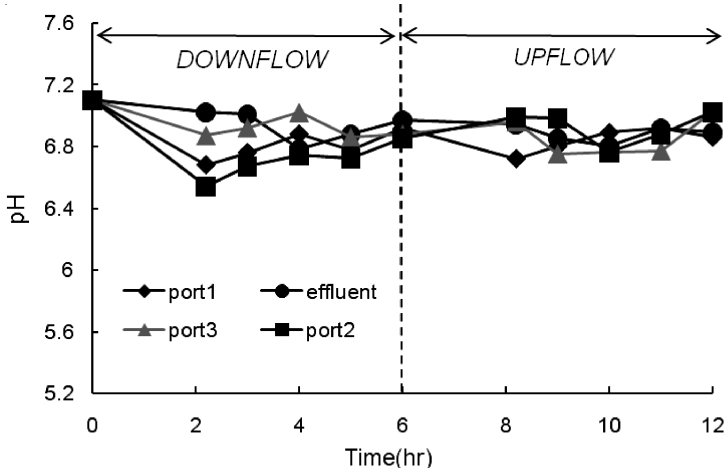

(a) New media

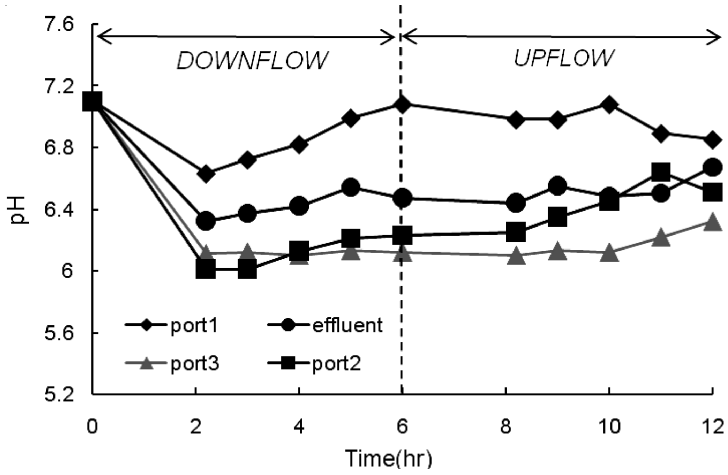

(b) Media from field

Fig. 10. Variation in pH at the different ports for the reactor filled with the new media and media taken from field on the downflow and upflow

The lower pH levels for the reactor operated with media taken from field appeared to compare to those of the new media, due to impurities that attached to the media during the filtration process. The decrease in the pH level was distinct within the initial 2.2 h and did not vary remarkably over time. The pH at port 2 during the initial 2.2 h was measured at 6.0 with the downflow operation, which was the lowest value during the operation period. After the initial great reduction of pH during 2.2 h at port 3, the pH value of the effluent after passage through the activated carbon did not change notably compared to other media after 2.2 h. The pH was 6.7 after the 12 h operation, which is a little lower than the initial pH of 7.1.

The variation in turbidity was simulated in Fig. 11 during operation of the two filtration systems for the filled with new media (a) and media from the field (b). The turbidity removal efficiency was measured to be 55 % through the layer of coarse sand and gravel at 2.2 h and removed *ca.* 91 % after 6 h for the new media filled filtration system. This system showed remarkably than 98 % for the removal of turbidity in the effluent. The turbidity removal reached more than 90 % for all sampling ports at 6 h and the efficiency increased to small extent when the flow direction changed to upflow. Especially, the sand layer had an important role to the removal of turbidity in this filtration system. More than 98% of the turbidity was eliminated with the new sand media for the 12 h operation.

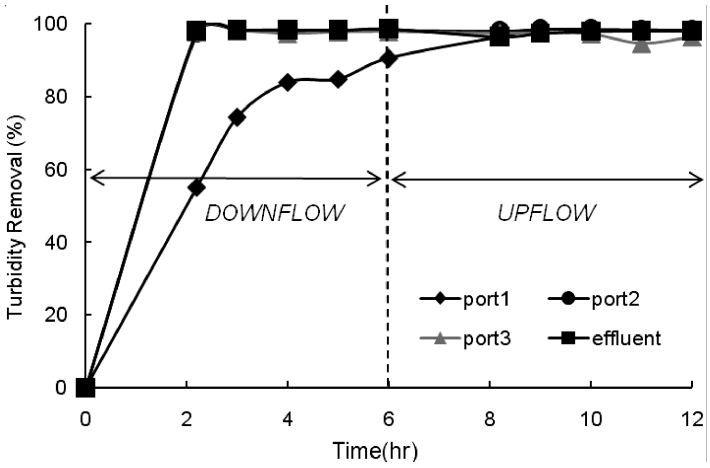

(a) New media

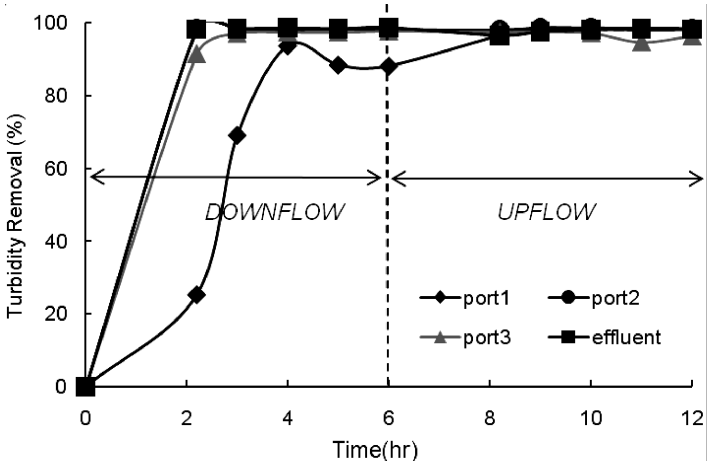

(b) Media from the field

Fig. 11. Removal efficiency of turbidity at the different ports for the reactor filled with the new media and media taken from field on the downflow and upflow

The removal efficiency of turbidity corresponded to the half value of that of the new one through sand layer filtration at 2.2 h for the field media. However, the removal efficiency reached a similar extent of new media in effluent through filtration of the all multi-media. The ability of turbidity removal for the filtration by the field media was fair after the flow direction was changed to upflow at 6 h. Generally, symptoms such as high turbidity in the effluent or clogging due to the accumulation of pollutants inside void in media because of turbid is occurred in the long run of filtration system without backwashing. However, in this case, variations in the sea tide were repeated in this inclined filtration system, so backwashing might be naturally practiced. This result showed that an inclined designed filtration system located in the seaside could run for a longer term without backwashing due to the effect of tide variation. The turbidity removal after passing activated carbon increased somewhat at all designed sampling times. However, the final removal efficiency was more than 98 % for the field media filtration system at the effluent. It was speculated that the functions of the serial media filtration system in the field was still fair for the removal of turbidity.

The removal efficiency for iron was presented with a reaction time to evaluate the effect of the filtration system in Fig. 12. More than 87 % of the iron was removed during 2.2 h at port 1 in the new media-filled filtration system, and more than 99 % at port 2; iron was not detected in the effluent. The filtration function in the sand layer for the removal of iron was good as well as turbidity. Almost all iron in the influent was removed after a series of filtrations with new media.

The removal of iron was effectively attained for the field media filtration system. Iron removal at port 1 during 2.2 h reached 51 %. A lower removal efficiency appeared than new media during the 2.2 h operation. But *ca.* 99 % removal efficiency was reached after passed through a series of field media after 6 h. The removal efficiency of iron was measured at 100 % in the effluent for the series filtration with field media.

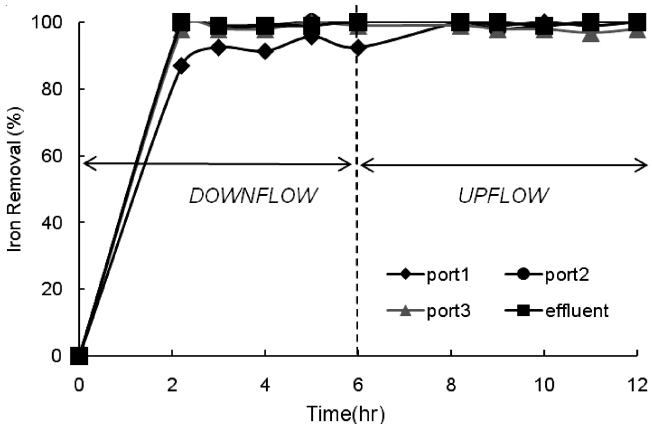

(a) New media

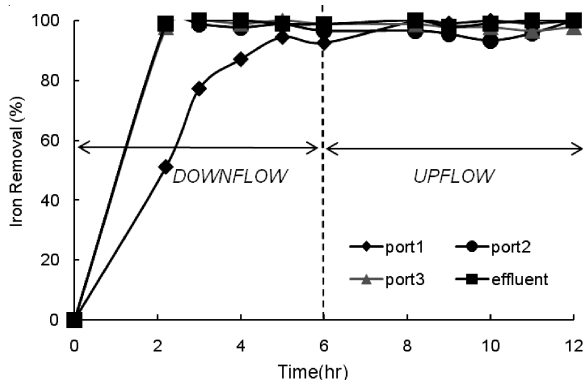

(b) Media from the field

Fig. 12. Removal efficiency of iron at the different ports for the reactor filled with the new media and media taken from field on the downflow and upflow

The tensile strength and permeability coefficient of non-woven fabric brought from the inclined filtration system was evaluated in this experiment and those values were compared to those of the new system. The tensile strength and permeability coefficient for non-woven fabric from the field did not show a big difference from new one. But the coefficient of permeability for the bentonite mat in the field was 2.2×10^{-3} cm/s, which was a much higher level compared to the new product. This result indicated that the impermeable function for the bentonite mat from the filtration system was weaker than the initial one, and perhaps physical damage to the bentonite occurred. The deterioration of the bentonite mat could have occurred at a high concentration of salt. In this case, various potential causes for the deterioration of bentonite mat exist, such as a high concentration of iron in the leached polluted soil, a change in the water retaining rate due to variations in the tide, increased water pressure due to the rising ground-water level during rainy season, or a high level of salt in the seawater. The decreased impermeable function was previously reported in the example of airport construction in Incheon due to unsuitable bentonite usage without considering the characteristics of seawater[17].

TABLE-2
COMPARISION OF TENSILE STRENGTH AND COEFFICIENT OF PERMEABILITY FOR THE NON-WOVEN FABRIC AND BENTONITE MAT

Item	Classification	Tensile strength (N)	Coefficient of permeability (cm/s)
Non-woven fabric P565	New product	482	4.8×10^{-2}
	Excavated product	424	1.8×10^{-2}
Non-woven fabric Tech 2800	New product	2752	4.1×10^{-2}
	Excavated product	2292	1.3×10^{-2}
Bentonite mat	New product	–	$<1 \times 10^{-7}$
	Excavated product	–	2.2×10^{-3}

Conclusion

This study was conducted to evaluate the causes of the high turbidity occurring around a slag landfill located by the seashore and to examine the function of the existing filtration system. The following conclusions were drawn from this research.

(1) Estimation of a possible pollution section were made effectively by the investigation with the measurement of electric specific resistance. Leakage was not found by the trace test with KBr for the upper section of the sheet file. Increased levels of iron and sulfate with an odor increase of hydrogen sulfide were observed at full tide. The initial black leakage water observed in the field gradually changed to white and then bluish green with the passage of time.

(2) The difference in filtration ability was not high for the new media and the excavated media from the field. Almost all iron was removed and the removal efficiency for the turbidity was more than 98 % through the multi-serial media filtration with coarse sand, activated carbon, fine sand and non-woven fabric.

(3) The lowered cutoff function of bentonite was found with the reaction of a high concentration of salt compared to the initial one. Black polluted soil was observed located around the bentonite mat during excavation. The materials used in landfills situated around the sea have to be carefully selected.

REFERENCES

1. W. Cha, J.W. Kim and H.C. Choi, *Water Res.*, **40**, 1034 (2006).
2. D.H. Choi, S.J. Maeng, D.C. Seo and D.H. Lee, *J. Korean Solid Wastes Eng. Soc.*, **12**, 429 (1995) (in Korean).
3. H. Shen and E. Forssberg, *Waste Manag.*, **23**, 933 (2003).
4. J. Yan, L. Moreno and I. Neretnieks, *Waste Manag.*, **20**, 217 (2000).
5. H. Shen and E. Forssberg, *Waste Manag.*, **23**, 933 (2003)
6. S.E. Kuh, K.J. Hwang and D.S Kim, *J. Korean Soc. Environ. Eng.*, **22**, 1139 (2000) (in Korean).
7. D.M. Proctor, K.A. Fehling, E.C. Shay, J.L. Wittenborn, J.J. Green, C. Avent, R.D. Bigham, M. Connolly, B. Lee, T.O. Shepker and M.A. Zak, *Environ. Sci. Technol.*, **34**, 1578 (2000).
8. J.O. Akinmusuru, *Resour. Conserv. Recycl.*, **5**, 73 (1991).
9. M. Maslehuddin, A.M. Sharif, M. Shameem, M. Ibrahim and M.S. Barry, *Construc. Build. Mater.*, **17**, 105 (2003).
10. D.G. Montgomery and G. Wang, *Cement Concrete Res.*, **22**, 755 (1992).
11. H. Motz and J. Geiseler, *Waste Manag.*, **21**, 285 (2001).
12. Y.Z. Lan, S. Zhang, J.K. Wang and R.W. Smith, *Acta Metal. Sinica*, **19**, 449 (2006) (English Letters).
13. X. Wang and Q.S. Cai, *Pedosphere*, **16**, 519 (2006).
14. J.M. Cha, J.Y. Kim, B.T. Lee, K.W. Kim and J.Y. Oh, *J. Korean Soc. Geo-system Eng.*, **37**, 327 (2000) (in Korean).
15. J.K. Kim, S.P. Hong, K.Y. Kim and Y.J. Cho, *J. Environ. Impact Assess.*, **13**, 223 (2004) (in Korean).
16. H.K. Lee and D.H. Lee, *J. Korean Soc. Environ. Eng.*, **27**, 75 (2005) (in Korean).
17. K.H. Lee, T.S. Huh and S.B. Yang, Technology Bulletin in Yooshin Engineering Corporation, 11, p. 181(2006) (in Korean).

(*Received*: 10 June 2009; *Accepted*: 31 October 2009) AJC-8004